ELSEVIER

Polymer 41 (2000) 9073–9080

polymer

www.elsevier.nl/locate/polymer

Thermal properties of poly(styrene-*block*-ϵ-caprolactone) in blends with poly(vinyl methyl ether)

W.Y. Yam[a], J. Ismail[a], H.W. Kammer[a], M.D. Lechner[b], C. Kummerlöwe[c,*]

[a]*School of Chemical Sciences, Universiti Sains Malaysia, 11800 Penang, Malaysia*
[b]*Physical Chemistry, University of Osnabrück, 49069 Osnabrück, Germany*
[c]*Fachbereich Werkstoffe und Verfahren, Fachhochschule Osnabrück, 49076 Osnabrück, Germany*

Received 15 December 1999; received in revised form 3 March 2000; accepted 5 April 2000

Abstract

The thermal characteristics of a styrene-ϵ-caprolactone diblock copolymer, P(S-*b*-CL), in blends with poly(vinyl methyl ether) (PVME) were studied by DSC. The glass transition temperatures show that PVME is only dissolved in the PCL block. It segregates from the PCL block at low temperatures. The addition of PVME leads to increasing crystallinity of the PCL block in a certain range of composition. However, degrees of crystallinity do not change significantly with crystallization temperature. Optical inspection revealed that the PCL block does not form spherulites. The crystallization kinetics of the PCL block has been systematically studied. The rate constants of crystallization for different blends decrease exponentially with crystallization temperature, whereas the rates of crystallization are scarcely affected by PVME content. The Avrami exponents were found close to two.

Keywords: Poly(styrene-*b*-ϵ-caprolactone); Poly(vinyl methyl ether); Polymer blends

1. Introduction

Polymer blends containing block copolymers as one component have found considerable scientific interest in recent years. Fields of application of block copolymers, among others, are compatibilization of polymer blends and impact modification. Hence, a growing number of papers on phase behavior, morphology and properties of blends of block copolymers with homopolymers can be found in literature.

The miscibility of a diblock copolymer, poly(A-*b*-B), with a corresponding homopolymer is mainly ruled by entropic effects. The homopolymer can only be dissolved in the corresponding block when its molar mass is smaller or equal to that of the block. If the block copolymer is blended with a homopolymer or a random copolymer, poly(C), which is miscible with one block, enthalpic effects may be considered as an additional driving force for miscibility [1]. It was found for blends of poly(2,6-dimethyl-1,4-phenylene oxide) (PPO) and poly(styrene-*b*-butadiene-*b*-styrene) (P(S-*b*-B-*b*-S)) [2–4] or poly(styrene-*b*-ϵ-caprolactone) (P(S-*b*-CL)) [5] that PPO is completely dissolved in the PS block. A more complex behavior was recently studied in Refs. [6,7]. Poly(styrene-*b*-isoprene) (P(S-*b*-I)) was blended with poly (vinyl methyl ether) (PVME). It is well established that homopolymer blends of PS and PVME are miscible and exhibit a lower critical solution temperature (LCST) [8,9]. For the system PVME/P(S-*b*-I), it was found that the PVME homopolymer was dissolved in PS microdomains and that upon heating PVME separates from the PS phase. Above the LCST two phases were observed, one block copolymer-rich phase, consisting of swollen microdomains, and one PVME-rich phase. Further temperature rise led to separated phases of the ordered block copolymer and the homopolymer that eventually turned into phases of disordered block copolymer and homopolymer.

Most studies are concerned with systems comprising block copolymers of amorphous blocks. Structure formation in symmetrical block copolymers with a crystallizable and an amorphous block results in alternating arrangement of crystalline and amorphous layers with the covalent links between them situated in the interfacial region. Examples for crystallizable blocks are poly(ethylene oxide) (PEO) [10–13] and poly(ϵ-caprolactone) (PCL) [13–19]. It is well known that PCL is miscible with numerous other homo- and copolymers [20] and, therefore, it is challenging to study the phase behavior and crystallization of blends containing the PCL as block of a block copolymer. The

* Corresponding author. Tel.: +49-541-969-2182; fax: +49-541-969-2999.
E-mail address: c.kummerloewe@fh-osnabrueck.de (C. Kummerlöwe).

0032-3861/00/$ - see front matter
PII: S0032-3861(00)00291-3

Table 1
Blend compositions

Blend number	Blend ratio of PVME/PS (wt%)	Blend ratio of PVME/PCL (wt%)	Blend ratio of PCL/ PVME + PS (wt%)
1 Block copolymer	0:100	0:100	56.4:43.6
2	8.0:92.0	6.2:93.8	54.6:45.4
3	25.7:74.3	20.9:79.1	49.3:50.7
4	40.9:59.1	34.6:65.4	43.6:56.4
5	51.0:49.0	44.3:55.7	39.1:60.9
6	58.1:41.9	51.4:48.6	35.4:64.6
7	75.7:24.3	70.4:29.6	24.1:75.9
8	87.4:12.6	84.1:15.9	14.2:85.8
9 PVME	100:0	100:0	0:100

crystallization behavior of a diblock copolymer with two crystallizable blocks, PCL and poly(2,2-dimethyl trimethylene carbonate) (P(CL-*b*-DTC)) was studied in Refs. [21,22] by applying a stepwise annealing procedure. This was done for both the block copolymer and in blends with the random copolymer poly(styrene-*co*-acrylonitrile) (SAN), where SAN is only miscible with the PCL block. It was found that crystallization of the blocks is strongly correlated resulting in reduced melting points of the blocks compared to that of the homopolymers. Moreover, dissolution of SAN in the PCL block leads to changes in crystallization behavior of both blocks. ten Brinke and coworker studied blends of PVME and poly(ϵ-caprolactone-*b*-trimethylene carbonate) (P(CL-*b*-TMC)) [23]. PVME is miscible with the PCL block. The PTMC block is not crystallizable. They found a microphase-separated morphology in the molten state, PVME residing inside PCL domains. During crystallization, space filling spherulites of the PCL block are growing in PVME/P(CL-*b*-TMC) blends [23]. PCL block spherulites of both the pure P(CL-*b*-TMC) block copolymer and in blends with PVME show distinct ring-shaped structures. Ring-banded spherulites have been observed in various miscible PCL homopolymer blends [24]. In contrast to the P(CL-*b*-TMC) block copolymer, no spherulitic structure could be found in P(S-*b*-CL) block copolymers [5]. In Ref. [17], it was shown that ring-banded spherulites are formed in triblock copolymers, P(S-*b*-B-*b*-CL), only if the PCL block and the PS block are separated by a sufficiently long polybutadiene block. In the P(CL-*b*-DTC) block copolymer, consisting of two crystallizable blocks, dendritic structures of the PDTC block and spherulites of the PCL block were observed during stepwise crystallization [21,22].

The present paper focuses on blends of PVME and a P(S-*b*-CL) block copolymer. PVME is in the molten state miscible with PCL and PS as well. The corresponding homopolymer blends are well examined [9,25,26]. Here, the crystallization of the PCL block in blends with PVME will be discussed and compared to previous results concerning PPO/P(S-*b*-CL) and PCL/PVME blends [5,26]. Also results on the phase behavior of blends of PVME and the block copolymer will be presented.

2. Experimental

2.1. Polymers

Commercial PVME (BASF) of molar mass $M_w = 81.8$ kg/mol ($M_w/M_n = 1.71$) was used in this study. The block copolymer, P(S-*b*-CL), was synthesized by anionic polymerization. The mole ratio of ϵ-caprolactone to styrene is 1.53 in the block copolymer. The molar mass of the block copolymer is 90 kg/mol and that of the PS block is 36 kg/mol. The polymer contains 10 wt% of PS homopolymer impurities.

2.2. Blend preparation

PVME and the block copolymer were dissolved separately in toluene. The polymer concentration of the stock solutions was 3 wt%. Different amounts of stock solutions were mixed and cast on glass slides. In this way, blends of different composition were prepared. The blend compositions are listed in Table 1. For the interpretation of glass transition data in terms of the Fox equation and degrees of crystallinity, it is necessary to calculate different blend ratios. The blend ratios "PVME/PS" give the weight fractions of PVME and PS, respectively, with reference to PVME and the total PS content of the blend, i.e. PS block plus PS homopolymer impurities, $m_{PVME}/(m_{PVME} + m_{PS\text{-}b} + m_{PS})$. The third column represents the analogous weight fractions of PVME and the PCL block, $m_{PVME}/(m_{PVME} + m_{PCL\text{-}b})$, while the last column gives the weight fractions of the PCL block and PVME plus the total PS content in the blends. The blends were carefully dried before use.

2.3. DSC measurements

DSC measurements were carried out with a Mettler DSC TA 3000 instrument calibrated by standard methods. The applied heating and cooling regimes for the determination of the glass transition temperatures and degrees of crystallinity, for isothermal crystallization and annealing experiments are summarized in Table 2. The experimental data

Table 2
DSC heating and cooling regimes

Step number	Regime 1: ordinary scanning		Regime 2: isothermal crystallization		Regime 3: annealing at −40°C	
	Step	Obtained data	Step	Obtained data	Step	Obtained data
1	Cooling, 20°C/min, 25 → −90°C		Heating, 20°C/min, 25 → 130°C		Heating, 20°C/min, 25 → 130°C	
2	Heating, 20°C/min, −90 → 130°C		Annealing, 10 min at 130°C		Annealing, 10 min at 130°C	
3	Annealing, 10 min at 130°C		Cooling, 20°C/min, 130°C → T_c		Cooling, 20°C/min, 130 → −40°C	
4	Cooling, 20°C/min, 130 → −90°C	T_c, Fig. 2	Annealing, $5t_{0.5}$ at T_c	$t_{0.5}$, Fig. 6; $X(t)$, Figs. 7 and 8	Annealing, 60 min at −40°C	
5	Heating, 20°C/min, −90 → 130°C	ΔH, Fig. 1; T_g, Fig. 3	Heating, 20°C/min, T_c → 130°C	T_m, Fig. 5; ΔH, Fig. 1	Cooling, 20°C/min, −40 → −90°C	
6					Heating, 20°C/min, −90 → 130°C	ΔH, Fig. 1; T_g, Fig. 4

obtained from the respective steps of the DSC measurements as well as the figures in which they are reported are documented in Table 2.

Isothermal crystallization experiments were carried out at crystallization temperatures, T_c, between 35 and 45°C. The samples were heated to 130°C and annealed at that temperature for 10 min to extinguish their thermal history. Then, the samples were cooled to their respective crystallization temperatures with a cooling rate of 20°/min and allowed to crystallize for five half-times of crystallization, $t_c = 5t_{0.5}$.

3. Results and discussion

3.1. Crystallinity of the PCL block

The crystallinity, X^*, of the PCL block was calculated from the enthalpy of melting ΔH by Eq. (1)

$$X^* = \frac{\Delta H}{w_{PCL} \cdot \Delta H_{ref}} 100\% \quad (1)$$

where w_{PCL} is the weight fraction of PCL in the blends (column 4 of Table 1) and $\Delta H_{ref} = 136.1$ J/g the reference melting enthalpy of 100% crystalline PCL [27].

The crystallinity X^* of the PCL block as a function of weight fraction of PVME with respect to the PCL block in the blends is shown in Fig. 1. It can be seen that the PCL block crystallinities depend on both the thermal history of the blends and the PVME weight fraction. Increasing the PVME content leads to higher PCL crystallinity. The crystallinity decreases dramatically only when the PVME weight fraction exceeds 50%. Increase of PCL crystallinity with increasing PVME content is also observed for homopolymer blends [25,26] and in blends of PVME and P(CL-*b*-TMC) block copolymer [23]. It might be concluded that PVME promotes the crystallization of PCL.

Fig. 1 exhibits clearly that the crystallinities of the samples, crystallized isothermally for five half-times of crystallization, are, at least for small PVME contents, remarkably lower than that obtained during cooling the samples with 20°/min from the melt to temperatures below 0°C. No significant differences can be observed when samples were isothermally crystallized at different temperatures, T_c. The solid line in Fig. 1 indicates a master curve calculated for all data obtained after regime 2. The crystallinity of the PCL block in the pure block copolymer crystallized isothermally remains at about 20% irrespective of crystallization temperatures. In contrast, the crystallinity of the PCL block in the pure block copolymer, crystallized according to regimes 1 and 3, reaches values above 30%. No significant difference can be detected between the crystallinities measured according to regimes 1 and 3.

It may be concluded that a certain part of PCL is not able to crystallize under isothermal conditions applied here and that cooling to lower temperatures than the applied isothermal crystallization temperatures favors crystallization. The

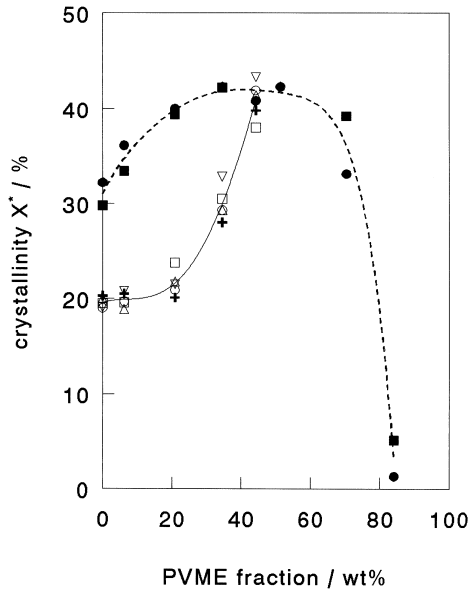

Fig. 1. Crystallinity of the PCL block of P(S-*b*-CL) as a function of PVME weight fraction (column 3 of Table 1). DSC regime 1: X. DSC regime 2: A, $T_c = 38°C$; +, $T_c = 39°C$; K, $T_c = 40°C$; L, $T_c = 41°C$; W, $T_c = 42°C$. DSC regime 3: B.

crystallization temperatures, T_c, detected during the cooling cycle of regime 1 are shown in Fig. 2. The crystallization occurs between 25 and 13°C and the T_c decreases with increasing PVME content. No crystallization during cooling with 20°/min can be observed in blends containing more than 50% PVME in relation to the PCL block. Blend 7 displays cold crystallization during reheating whereas the PCL block in blend 8 does not crystallize at all.

During the examination of the P(S-*b*-CL) block copolymer by optical microscopy, no crystalline structures could be found. PCL spherulites emerging from the PCL blocks in block copolymers were found in P(CL-*b*-DTC) diblock copolymers and blends with SAN [22], as well as in P(CL-*b*-TMC) and blends with PVME [23]. The PCL block crystallizes under these conditions from a mixed melt with SAN and PVME, respectively. The block copolymers differ in their polycarbonate blocks. PDTC is crystallizable with a crystallization temperature above that of the PCL block whereas PTMC is amorphous and its glass transition is below the crystallization temperature of the PCL block. The amorphous PTMC block does not hinder PCL crystallization by vitrification. In the present P(S-*b*-CL) block copolymer, the glass transition of the PS block is higher than the crystallization temperature of the PCL block and obviously prevents spherulite formation. The observation is in agreement with studies on the triblock copolymer P(S-*b*-B-*b*-CL) [17] which revealed that PCL spherulites were only observed when the PCL block and the PS block are separated by a sufficiently long PB-mid block.

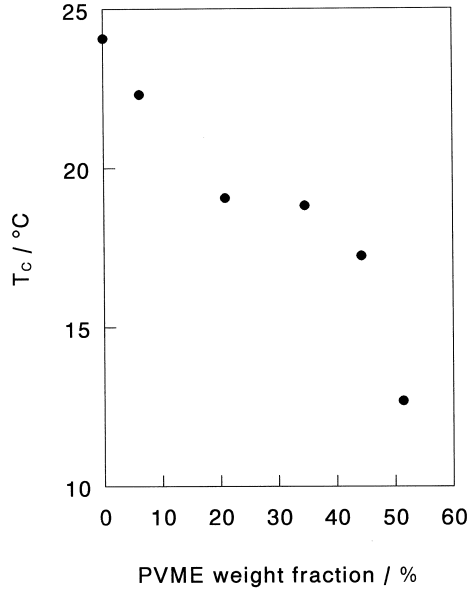

Fig. 2. Crystallization temperature of the PCL block obtained while cooling samples from the melt with 20°/min as a function of PVME weight fraction (column 3 of Table 1).

3.2. Glass transition temperatures

The glass transition temperatures of the PVME/P(S-*b*-CL) blends, measured in the second heating cycle of regime 1 (cf. Table 2), are summarized in Fig. 3 as a function of the weight fraction of PVME with respect to either the total PS content or the PCL-block content in the blends.

The pure block copolymer exhibits two glass transition temperatures, for the PCL phase $T_{g,PCL} = -63.5°C$ and for the PS phase $T_{g,PS} = 104.4°C$. The glass transition temperature of PVME is $T_{g,PVME} = -23.8°C$. These values were used to calculate the glass transition temperatures of the blends according to the Fox equation

$$\frac{1}{T_g} = \frac{w_1}{T_{g1}} + \frac{w_2}{T_{g2}} \tag{2}$$

where quantities w_i denote the weight fractions of PVME and the respective second component and $T_{g,i}$ the corresponding glass transition temperatures. The calculated values are indicated by solid lines in the diagram. The results of crystallinity measurements discussed above show that a remarkable part of the PCL block is crystalline. Therefore, the weight fraction of PVME was corrected and the T_g values, indicated by open symbols in Fig. 3, correspond to the PVME weight fractions in relation to the amorphous part of the PCL block. Good agreement between the calculated and experimental glass transitions may be recognized for the PVME/PCL mixtures. The glass transitions of the PS phase do not follow the Fox equation with increasing PVME content. Only for two blends a slight decrease of the glass transition of PS phase can be observed. These results indicate that PVME is mainly situated in the PCL phase. PCL block and PVME form a mixed phase. The PS block seems to be hidden by the PCL phase and is not accessible

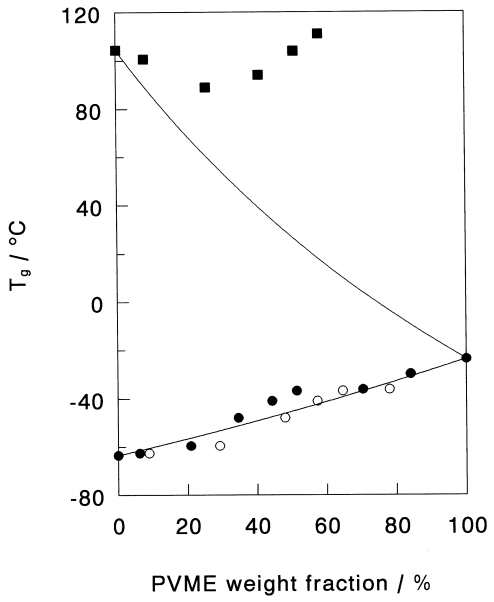

Fig. 3. Glass transition of the PVME/P(S-*b*-CL) blends measured according to regime 1 in Table 2. Solid curves are calculated after Fox equation. B T_g of PS phase, blend ratio, column 2 of Table 1; X T_g of PCL phase, blend ratio, column 3 of Table 1; W T_g of PCL phase, blend ratio corrected with respect to crystallinity of PCL (cf. text).

for PVME. For the PVME/P(CL-*b*-TMC) blends studied by ten Brinke et al. [23], it was shown by modulated DSC measurements that two glass transition temperatures, one of a PCL block-rich phase and one of a PVME-rich phase, could be detected in the range of higher PVME contents, leading to the conclusion that PVME segregates to some extent from the PCL domains. The results presented so far for the PVME/P(S-*b*-CL) blends do not allow such a conclusion.

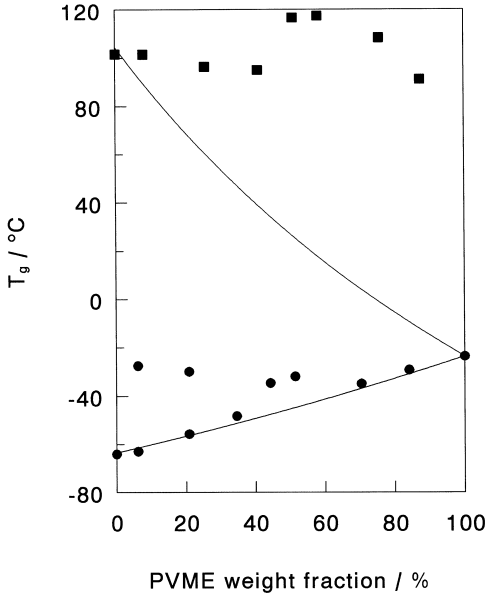

Fig. 4. Glass transition of the PVME/P(S-*b*-CL) blends measured according to regime 3 of Table 2. Solid lines are calculated after Fox equation. B T_g of PS phase, blend ratio, column 2 of Table 1; X T_g of PCL phase, blend ratio, column 3 of Table 1.

In our previous study concerning the homopolymer blends [26], we found that the glass transition temperature T_g can be adequately described by the Fox equation over the whole range of composition for blends, rapidly quenched from the melt to −75°C and reheated immediately to determine the glass transition. Therefore, the results of Fig. 3 are consistent with those for homopolymer blends. However, homopolymer blends, quenched from the melt to −40°C and annealed there for 1 h, exhibit a different behavior. In the range of blend compositions, where the glass transition is below the annealing temperature, the chains are mobile enough to use the annealing time for further phase separation. This results in increasing T_g and deviations from the Fox equation as well as in slightly higher crystallinity of the PCL homopolymer. In the block copolymer blends under discussion, no further increase of crystallinity occurs when DSC regime 3 was applied. The glass transition temperatures, measured according to regime 3, are depicted in Fig. 4. It becomes obvious that the glass transition temperatures of the blends, comprising less than 60 wt% of PVME, deviate from the Fox equation. In blends with high PCL block content even the T_g of the PCL block can be detected. Annealing at −40°C leads to segregation of the PCL block and PVME and occurrence of PVME-rich and PCL block-rich phases. Again, the glass transition of the PS block remains unchanged with increasing PVME content.

Previous studies revealed [9] that phase separation of PVME and PS homopolymers is expected to occur in the same temperature range where samples were annealed during the DSC measurements. Therefore, the question arises whether PVME separates from the PS-block during the procedure of DSC measurement. A careful inspection of the first heating run of as-cast samples showed merely a nearly constant T_g of the pure PS phase. In addition, PVME/P(S-*b*-CL) blends were annealed at temperatures between 80 and 120°C. Again, the glass transition temperature of the PS block did not change after annealing. These results indicate that the PS phase of the solution cast samples does not contain PVME. In other words, the PS phase of the block copolymer seems to be not accessible for PVME.

In conclusion, the studies of glass transition temperature suggest that in the PVME/P(S-*b*-CL) blends under discussion, PVME only mixes with the PCL block. It is likely that the microphases of PS are surrounded by the PCL block. This arrangement may prevent access of PVME to the PS block. Segregation of PVME and the PCL block occurs at low temperatures, however, does not lead to significantly enhanced crystallinity of the PCL block.

3.3. Isothermal crystallization of the PCL block

Isothermal crystallization experiments were carried out according to regime 2 (cf. Table 2). In order to impose

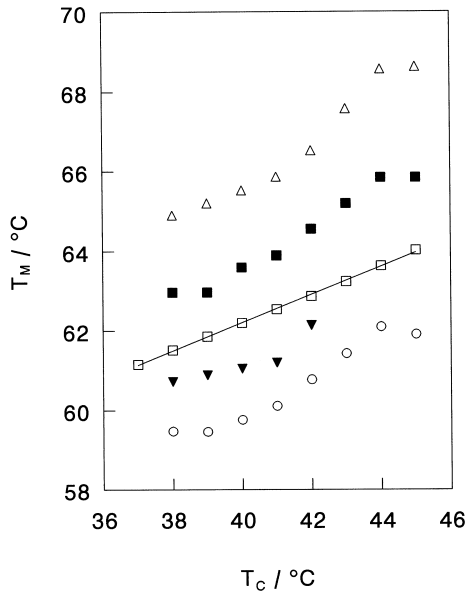

Fig. 5. Melting temperature of the PCL block in the PVME/P(S-*b*-CL) blends as a function of crystallization temperature. Data points are displaced. W block copolymer, original position; K blend 2, displaced by +5°C; A blend 3, displaced by +2°C; B blend 4, displaced by +1°C; P blend 5, original position.

comparable thermal histories to all blends, isothermal crystallization experiments require determination of the half-time of crystallization, $t_{0.5}$, defined as the time taken for half of the crystallinity to develop. The half-time of crystallization was measured for each crystallization temperature, T_c.

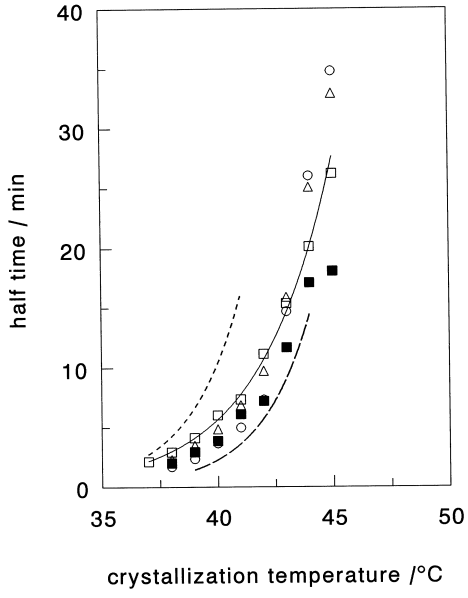

Fig. 6. Half-time of crystallization versus crystallization temperature, blend numbers according to Table 1. The solid curve refers to blend 3 (marker A). The dashed and dotted curves represent the homopolymer PCL and the 80:20 PCL/PVME blend, respectively. W block copolymer; K blend 2; B blend 4.

The Hoffman–Weeks plots of PVME/P(S-*b*-CL) blends are presented in Fig. 5. The melting temperatures were measured after the samples were crystallized for five half-times at the respective crystallization temperatures. The figure shows that the equilibrium melting points cannot be reliably determined, due to scatter of the data, except for blend 3 (correlation 0.999). Extrapolation results in $T_m^0 = 71$°C for that blend which is in good agreement with $T_m^0 = 73$°C for the homopolymer PCL [26].

To study the overall crystallization kinetics of the blends the Avrami equation was used:

$$X(t) = 1 - \exp[-K_A(t - t_0)^{n_A}] \quad (3)$$

where $X(t)$ represents the ratio of the degree of crystallinity at time t and the final degree of crystallinity and is calculated as ratio of crystallization peak areas of isothermal experiments, $A(t)/A(\infty)$. Quantities K_A and n_A are the overall rate constant of crystallization and the Avrami exponent, respectively; t_0 represents the induction period which was determined experimentally and defined as the period of time after which first deviations of the DSC trace from the base line could be detected.

Fig. 6 presents the half-times of crystallization as a function of crystallization temperature for different blend compositions. The half-times increase exponentially with ascending crystallization temperature. One observes that the rate of crystallization, $t_{0.5}^{-1}$, for the block copolymer does not change significantly with PVME content. For comparison, the half-times of crystallization for homopolymer PCL and in a 80:20 PCL/PVME blend are also indicated in Fig. 6 [26]. It becomes obvious that the rate of crystallization, $t_{0.5}^{-1}$, in a certain range of crystallization temperatures is highest for the PCL homopolymer and decreases in blends with PVME. The rate of crystallization of the PCL block is in between that of the homopolymer PCL and the PCL/PVME blends. A different behavior was observed in blends of P(CL-*b*-DTC) and SAN where SAN is only miscible with the PCL block [21,22]. The rate of crystallization of the PCL block slowed down with increasing SAN content. These differences are ruled by the glass transition temperature of the amorphous component that has to be rejected from the growing crystallites. Moreover, the rate of crystallization of the PCL block decreases also in blends of the P(S-*b*-CL) block copolymer and PPO where PPO is only miscible with the PS block [5]. Addition of PPO leads to ascending glass transition temperature of the PS block mixed with PPO.

Examples of Avrami plots are shown in Fig. 7 for blends crystallized at 42°C. Linear relationships can be seen that allow to estimate parameters K_A and n_A from the plots. The accuracy of the regression coefficients were analyzed in terms of a statistical *t*-test at 95% confidence interval. Table 3 summarizes the results for $T_c = 42$ and 44°C. Avrami exponents n_A are approximately two. Similar results have been found for other block copolymers and their blends [5,22] whereas the Avrami exponent for homopolymers and

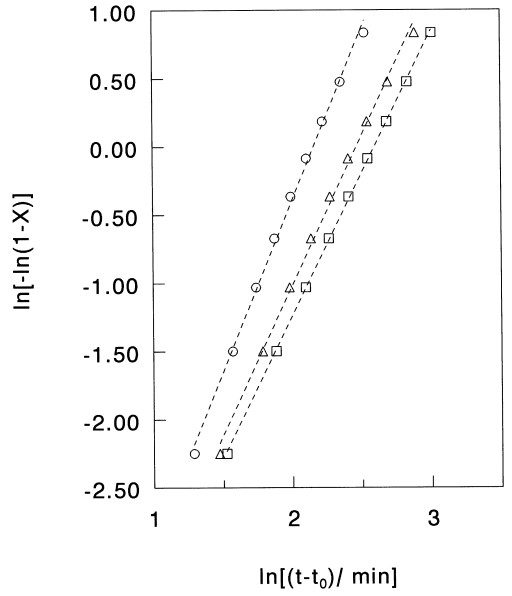

Fig. 7. Avrami plots for the PVME/P(S-*b*-CL) blends crystallized at 42°C, markers as in Fig. 6.

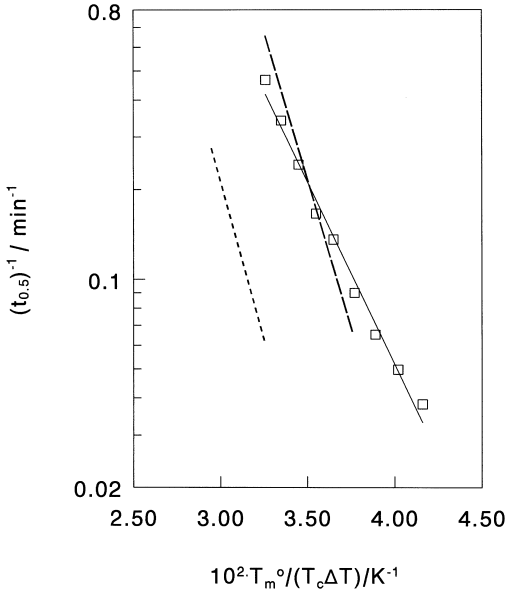

Fig. 8. Semilogarithmic plot of $t_{0.5}^{-1}$ versus $T_m^0/T_c\Delta T$. PCL—dashed curve; 70:30 PCL/PVME blend—dotted curve; blend 3—solid curve.

homopolymer blends is usually close to three [26]. This reduction of Avrami exponent might be due to restrictions in nucleation and growth imposed by the second block. The rate constants K_A do not change markedly with increasing PVME content. Only blend 4 displays some deviation.

The rates of crystallization, $t_{0.5}^{-1}$, may also be examined in a simplified version of the kinetic theory of crystallization [28]. It is assumed that the temperature dependence of the rate of crystallization follows an Arrhenius-like relation

$$\ln(t_{0.5}^{-1}) \propto -K_g \frac{T_m^0}{T_c \cdot \Delta T} \quad (4)$$

where K_g is the temperature coefficient of the crystallization process and ΔT is the undercooling. As Fig. 5 shows, we could only determine the equilibrium melting temperature T_m^0 for blend 3. Semilogarithmic plots of $t_{0.5}^{-1}$ after Eq. (4) are given in Fig. 8 for block copolymer blend 3, homopolymer PCL, and the 70:30 PCL/PVME blend. Undercooling ΔT was calculated using the equilibrium melting temperatures $T_m^0 = 71$, 73, and 75°C for blend 3, PCL and the 70:30 PCL/PVME blend [26], respectively. The rate of crystallization changes exponentially with $T_m^0/T_c\Delta T$. The temperature coefficients K_g are listed in Table 4. The confidence intervals are again at 95% confidence level. As can be seen, the constant K_g is greater for the homopolymer and the homopolymer blend than for the blend with the block copolymer. This reflects the same tendency as shown in Fig. 6 for the temperature dependence of the half-times.

Table 3
Avrami parameters for kinetics of crystallization of the PCL block in PVME/P(S-*b*-CL) blends at 42 and 44°C

Blend number after Table 1	n_A	K_A (10^3 min$^{-n_A}$)	$t_{0.5}$ (min)	r[a]
At $T_c = 42$°C				
1	2.5 ^ 0.1	4 ^ 1	7.3	0.999
2	2.2 ^ 0.1	5 ^ 1	9.7	0.999
3	2.08 ^ 0.03	4.5 ^ 0.3	11.1	0.9999
4	2.1 ^ 0.1	10 ^ 3	7.2	0.997
5	2.2 ^ 0.1	4 ^ 2	9.9	0.995
	n_A	K_A (10^4 min$^{-n_A}$)	$t_{0.5}$ (min)	r[a]
At $T_c = 44$°C				
1	2.48 ^ 0.1	2.7 ^ 0.6	23.3	0.999
2	2.2 ^ 0.2	7 ^ 5	25.1	0.992
3	2.5 ^ 0.2	4 ^ 2	20.1	0.997
4	2.1 ^ 0.2	20 ^ 10	17.1	0.992

[a] Correlation coefficient.

Table 4
Temperature coefficient K_g of Eq. (4)

Sample	K_g/K	r^a
PCL	200 ^ 10	0.999
PCL/PVME (70:30)	210 ^ 20	0.998
Blend 3	120 ^ 10	0.995

[a] Correlation coefficient.

4. Conclusions

In conclusion, the glass transition temperatures have been studied in blends of the block copolymer P(S-*b*-CL) with PVME by DSC, applying different heating and cooling regimes. It turned out that PVME does not mix with the PS block whereas it is dissolved in the PCL block. However, PVME segregates from the PCL block after annealing at low temperatures. The crystallization characteristics of the PCL block are influenced by PVME. The crystallinities after nonisothermal and isothermal crystallization increase with increasing PVME content in a certain range of PVME concentration. However, the degrees of crystallinities do not change significantly with crystallization temperature. Optical inspection revealed that the PCL block does not form spherulites. Investigation of crystallization kinetics shows that PVME does not influence markedly the crystallization of the PCL block. The temperature coefficient, characterizing the crystallization process, was found to be lower in blends of P(S-*b*-CL) and PVME than for the homopolymer PCL.

Acknowledgements

W.Y.Y. thanks the German Academic Exchange Service (DAAD) for a grant supporting her research stay in Osnabrück. This study was also supported by a research grant from Universiti Sains Malaysia at Penang.

References

[1] Adedeji A, Hudson SD, Jamieson AM. Polymer 1997;38:737.
[2] Trucker PS, Paul DR. Macromolecules 1988;21:2801.
[3] Trucker PS, Barlow JW, Paul DR. Macromolecules 1988;21:1678.
[4] Trucker PS, Barlow JW, Paul DR. Macromolecules 1988;21:2794.
[5] Kummerlöwe C, Martuscelli E, Kammer HW, Pauly St. Polym Networks Blends 1995;5:27.
[6] Lee Hwan-Koo, Kang Chang-Kwon, Zin Wang-Cheol. Polymer 1996;37:287.
[7] Lee Hwan-Koo, Kang Chang-Kwon, Zin Wang-Cheol. Polymer 1997;38:1595.
[8] Ubrich JM, Ben Cheikh Labri F, Monnerie L, Bauer BJ, Han CC. Macromolecules 1986;19:810.
[9] Tröger J, Kammer HW. Acta Polymerica 1992;43:331.
[10] Gervais M, Gallot B, Jerome R, Teyssie P. Makromol Chem 1981;182:989.
[11] Kuo WF, Tong SN, Pearce EM, Kwei TK. J Appl Polym Sci 1993;48:1297.
[12] Perret R, Skoulios A. Makromol Chem 1972;162:147 (see also p. 163).
[13] Gan Z, Zhang J, Jiang B. J Appl Polym Sci 1997;13:1763.
[14] Nojima S, Nakano H, Ashida T. Polymer 1993;34:4168.
[15] Nojima S, Hashizume K, Rohadi A, Sasaki S. Polymer 1997;38:2711.
[16] Nojima S, Kato K, Yamamoto S, Ashida T. Macromolecules 1992; 25:2237.
[17] Balsamo V, von Gyldenfeldt F, Stadler R. Macromol Chem Phys 1996;197:3317.
[18] Bogdanov B, Vidts A, van den Bulke A, Verbeek R, Schacht E. Polymer 1998;39:1631.
[19] Nojima S, Tanaka H, Rohadi A, Sasaki S. Polymer 1998;39:1727.
[20] Kammer HW, Kummerlöwe C. Adv Polym Blends Alloys Tech, vol. 5. Lancaster, PA; Basel: Technomic Publishers, 1994. p. 132.
[21] Kummerlöwe C, Morgenstern U, Kammer HW, Keul H, Höcker H. Polym Networks Blends 1993;3:137.
[22] Kummerlöwe C, Kammer HW, Androsch R, Radusch H-J. Polym Networks Blends 1994;4:1.
[23] Luyten MC, Bögels EJF, Alberda van Ekenstein GOR, ten Brinke G, Bras W, Komanschek BE, Ryan AJ. Polymer 1997;38:509.
[24] Kummerlöwe C, Kammer HW. Polym Networks Blends 1995;5:131.
[25] Oudhuis AACM, Thiewes HJ, van Hutten PF, ten Brinke G. Polymer 1994;35:3936.
[26] Yam WY, Ismail J, Kammer HW, Schmidt H, Kummerlöwe C. Polymer 1999;40:5545.
[27] Khambatta FB, Warner F, Russel T, Stein RS. J Polym Sci, Polym Phys Ed 1976;14:1391.
[28] Hoffman JD. Polymer 1982;24:3.